

Supporting information

Subnanometric CoSn clusters Embedded N-doped Carbon Nanobox (SN-CoSn@C NBs) Realizes High Efficiency Adsorption-Conversion of Polysulfide

Ruili Gao,^{‡a} Qian Zhang,^{‡a} Hui Wang,^{*a} Xuyun Wang,^a Jianwei Ren^{*b} and Rongfang Wang^{*a}

^aState Key Laboratory Base for Eco-Chemical Engineering, College of Chemical Engineering, Qingdao University of Science and Technology, Qingdao, 266042, China

email: wangh@qust.edu.cn (H. Wang) rfwang@qust.edu.cn (R. Wang)

^bDepartment of Mechanical Engineering Science, University of Johannesburg, Cnr Kingsway and University Roads, Auckland Park, 2092, Johannesburg, South Africa

email: jren@uj.ac.za (J. Ren)

[‡]Ruili Gao and Qian Zhang contributed to this work equally.

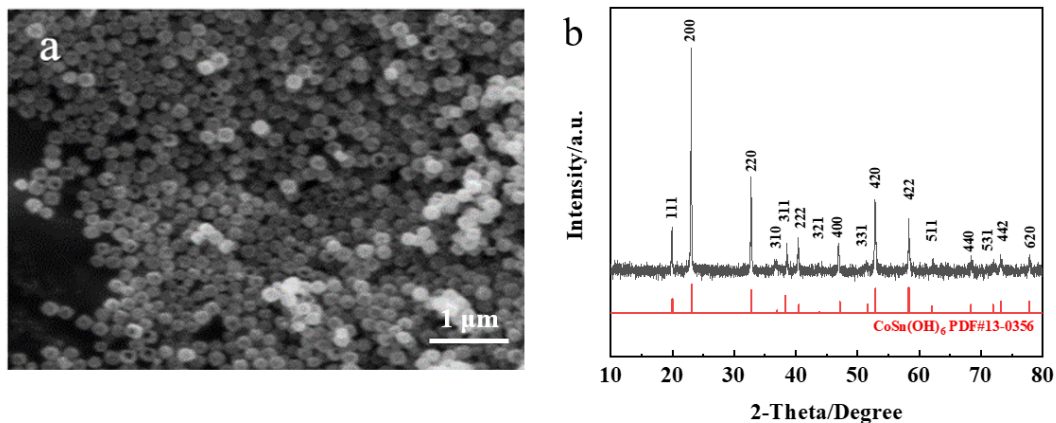


Fig. S1. SEM image and XRD pattern of the CoSn(OH)₆ sample.

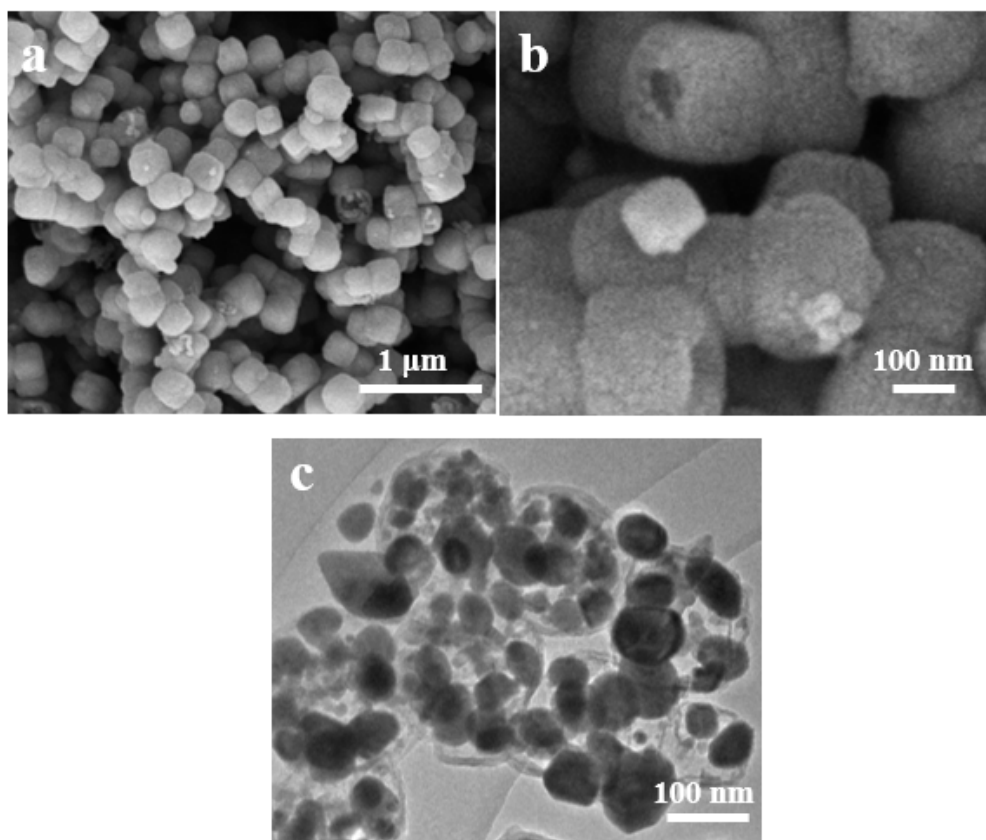


Fig. S2. (a, b) SEM and (c) TEM images of the $\text{CoSnO}_x@\text{C}$ NBs sample.

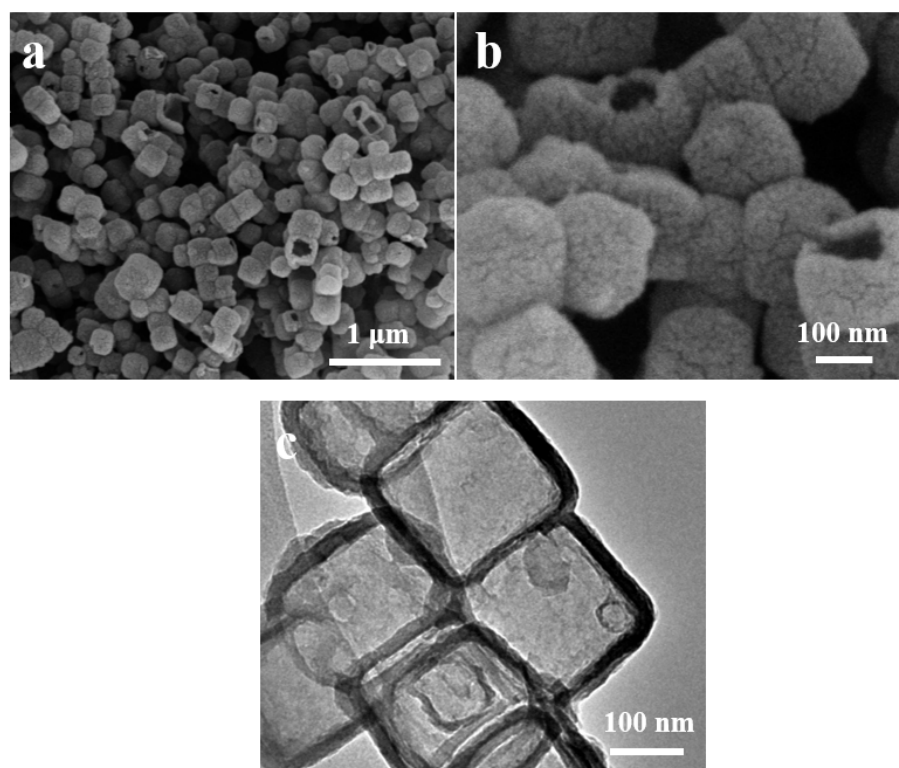


Fig. S3. (a, b) SEM and (c) TEM images of the $\text{CoSn}@\text{C}$ NBs sample.

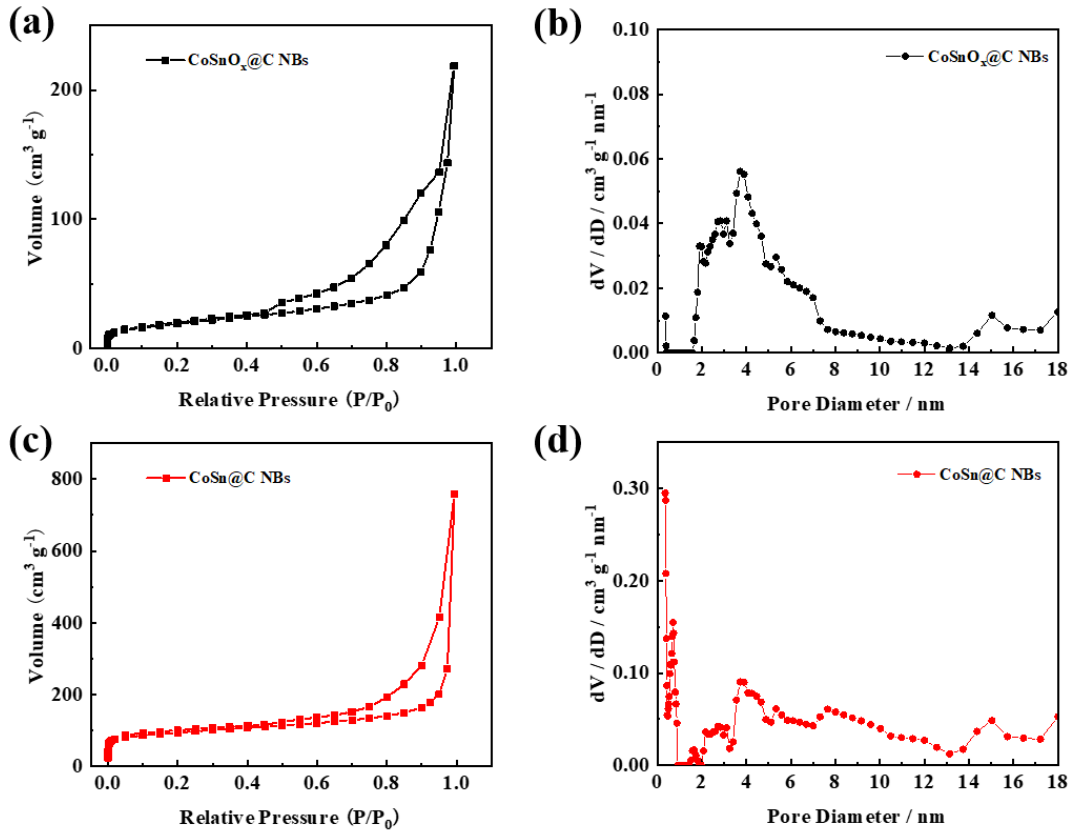


Fig. S4. (a) N₂ sorption isotherm and (b) pore-size distribution (PSD) of the CoSnO_x@C NBs sample. (c) N₂ sorption isotherm and (d) pore-size distribution (PSD) of the CoSn@C NBs sample.

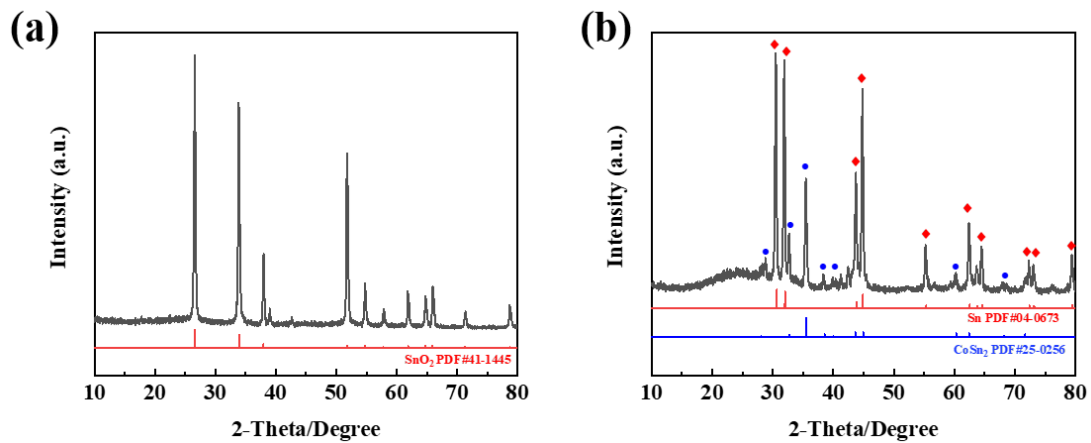


Fig. S5. XRD patterns of (a) after 6 M H₂SO₄ etching, and (b) after H₂ reduction.

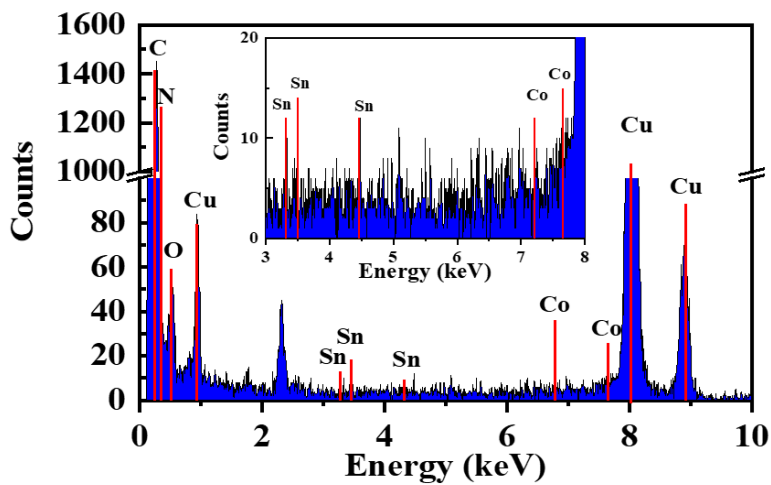


Fig. S6 EDS spectra of the SN-CoSn@C NBs sample.

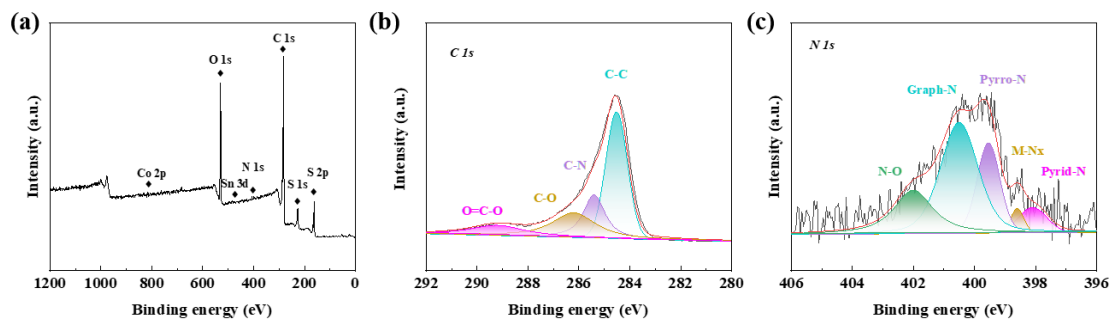


Fig. S7. (a) XPS spectrum, (b) high-resolution C *1s* and (c) N *1s* XPS spectrum of the SN-CoSn@C NBs sample.

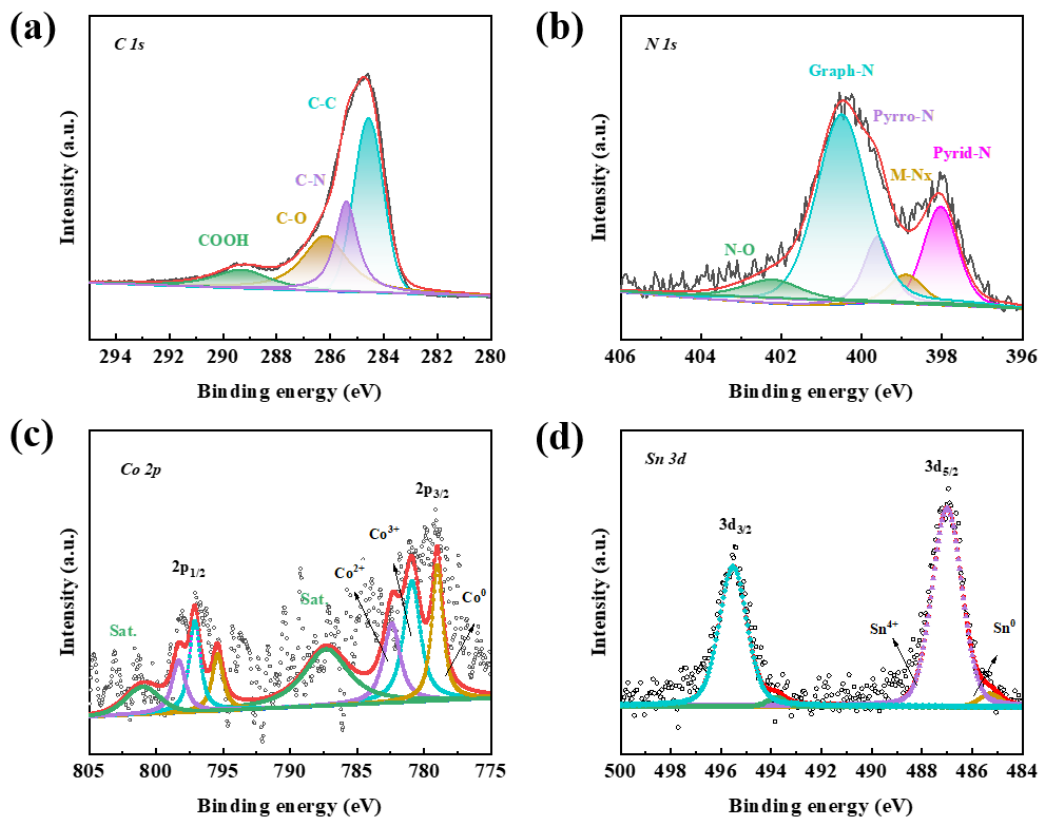


Fig. S8. High-resolution XPS spectra of the CoSn@C NBs sample: (a) C 1s, (b) N 1s (c) Co 2p and (d) Sn 3d.

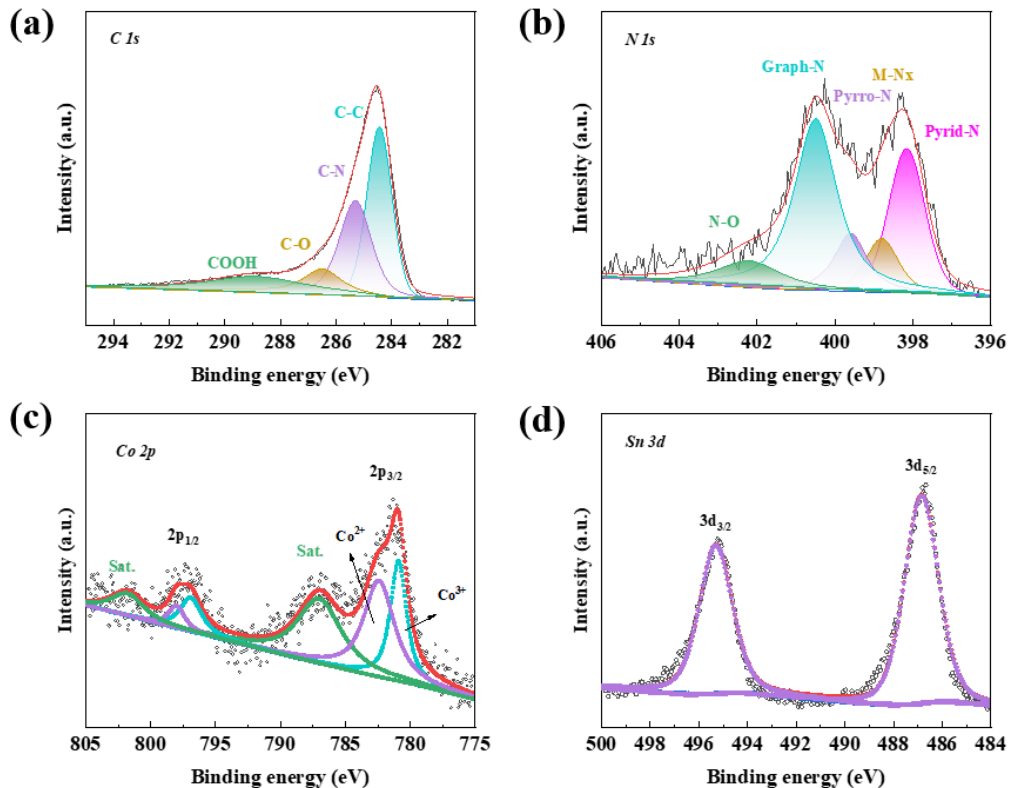


Fig. S9. High-resolution XPS spectra of the CoSnO_x@C NBs sample: (a) C 1s, (b) N

Is (c) Co 2p and (d) Sn 3d.

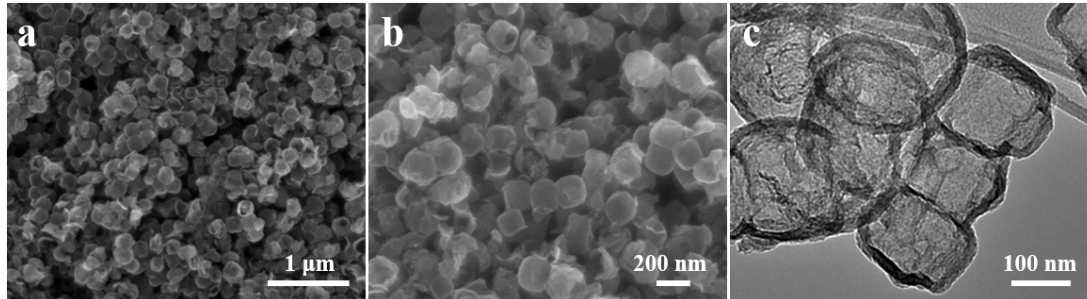


Fig. S10. (a, b) SEM and (c)TEM images of the CoSn@C NBs/S sample.

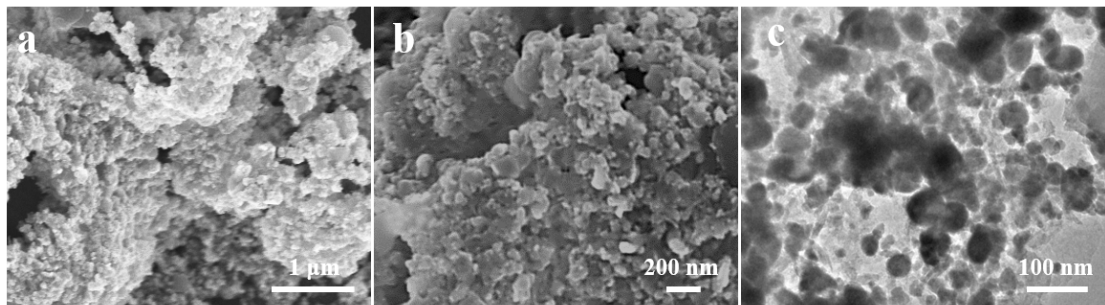


Fig. S11. (a, b) SEM and (c) TEM images of the CoSnO_x@C NBs/S sample.

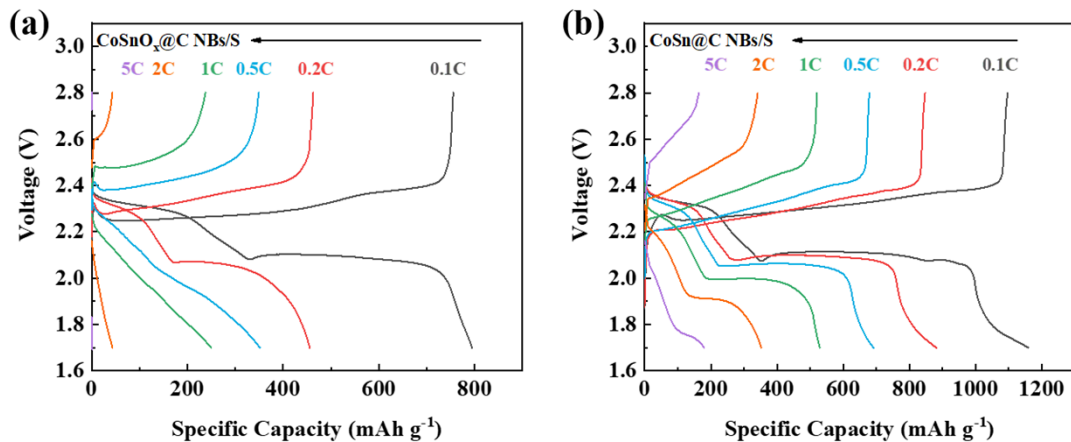


Fig. S12. The charge-discharge curves of (a) CoSnO_x@C NBs/S and (b) CoSn@C NBs/S electrodes at different current densities.

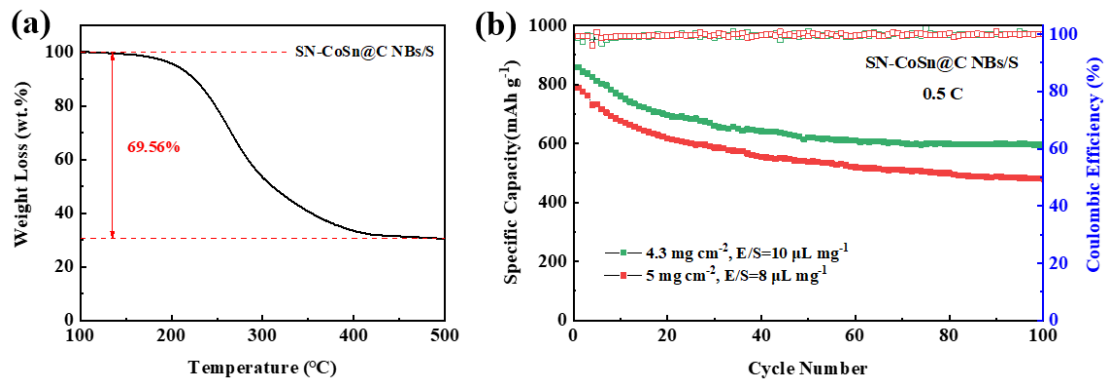


Fig. S13. (a) TGA analysis of the SN-CoSn@C NBs/S sample with 70% S-loading. (b) Cycling stability of SN-CoSn@C NBs/S electrode at 0.5 C: sulfur loading of 4.3 mg cm⁻², E/S=10 μL mg⁻¹ and 5 mg cm⁻², E/S=8 μL mg⁻¹.

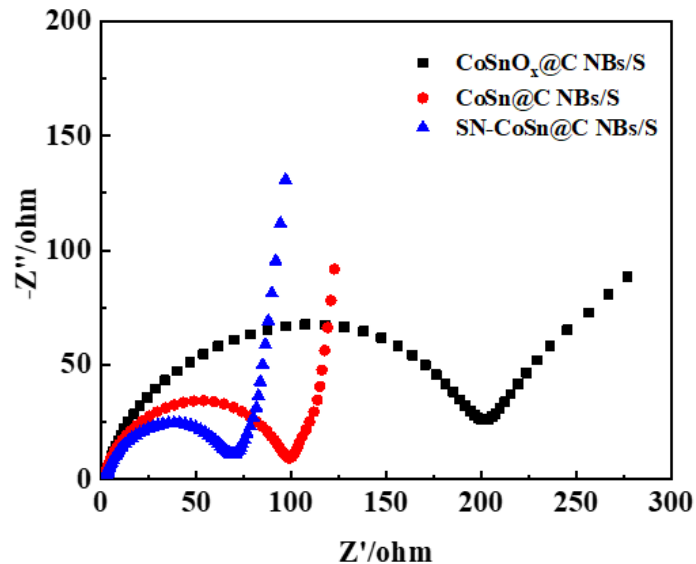


Fig. S14. EIS curves of the CoSnO_x@C NBs/S, CoSn@C NBs/S and SN-CoSn@C NBs/S samples.

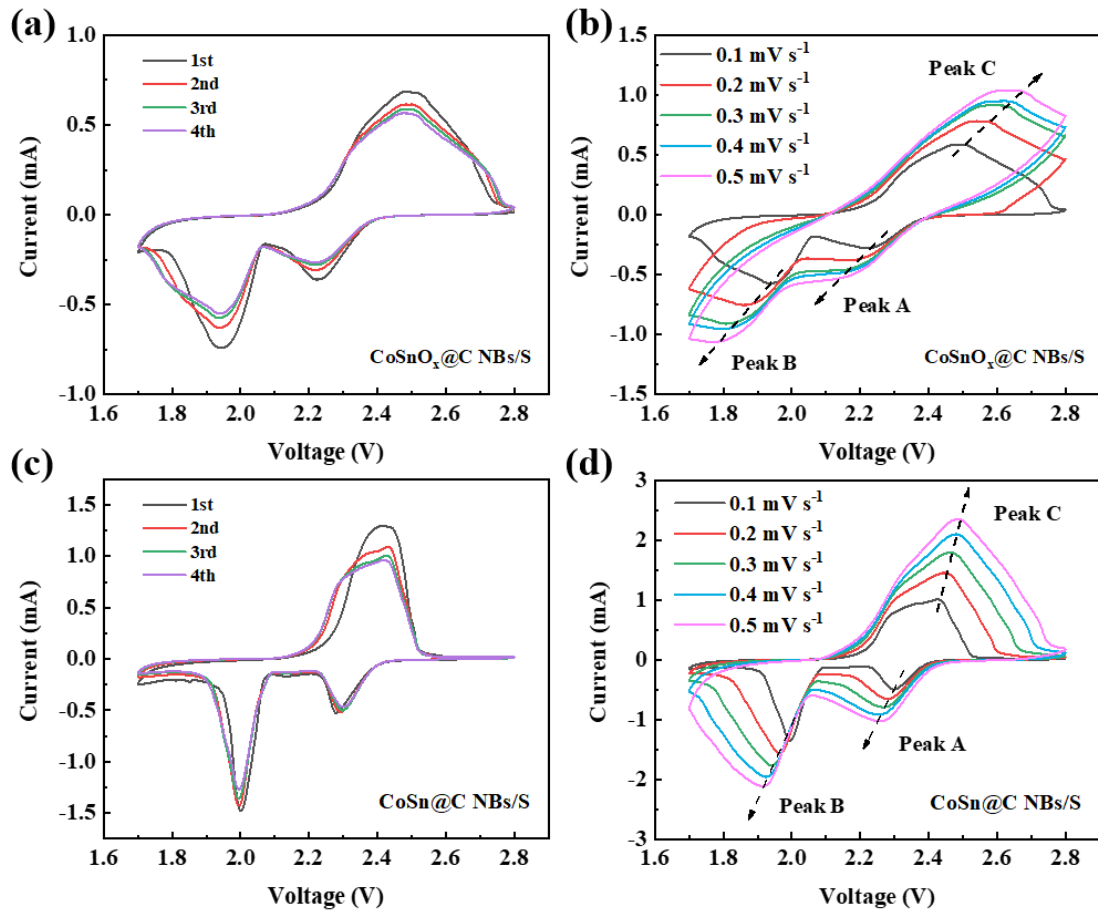


Fig. S15. CV curves of the $\text{CoSnO}_x@\text{C NBs/S}$ sample: (a) 0.1 mV s^{-1} and (b) $0.1\text{-}0.5 \text{ mV s}^{-1}$. CV curves of the $\text{CoSn}@ \text{C NBs/S}$ sample: (c) 0.1 mV s^{-1} and (d) $0.1\text{-}0.5 \text{ mV s}^{-1}$.

Table S1. Li^+ diffusion coefficients of the $\text{CoSnO}_x@\text{C NBs/S}$, $\text{CoSn}@ \text{C NBs/S}$ and $\text{SN-CoSn}@ \text{C NBs/S}$ three samples.

$D_{\text{Li}^+}(\text{cm}^2 \text{s}^{-1})$	A(cathodic peak)	B(cathodic peak)	C(anodic peak)
	$\text{S}_8 \rightarrow \text{LiPS} (\text{Li}_2\text{S}_n, 4 \leq n \leq 8)$	$\text{LiPS} (\text{Li}_2\text{S}_n, 2 \leq n < 4) \rightarrow \text{Li}_2\text{S}_2/\text{Li}_2\text{S}$	$\text{Li}_2\text{S}_2/\text{Li}_2\text{S} \rightarrow \text{LiPS} \rightarrow \text{S}_8$
$\text{CoSnO}_x@\text{C NBs/S}$	5.03×10^{-10}	1.62×10^{-9}	1.43×10^{-9}
$\text{CoSn}@ \text{C NBs/S}$	2.04×10^{-9}	4.31×10^{-9}	1.33×10^{-8}
$\text{SN-CoSn}@ \text{C NBs/S}$	7.02×10^{-9}	1.88×10^{-8}	4.33×10^{-8}

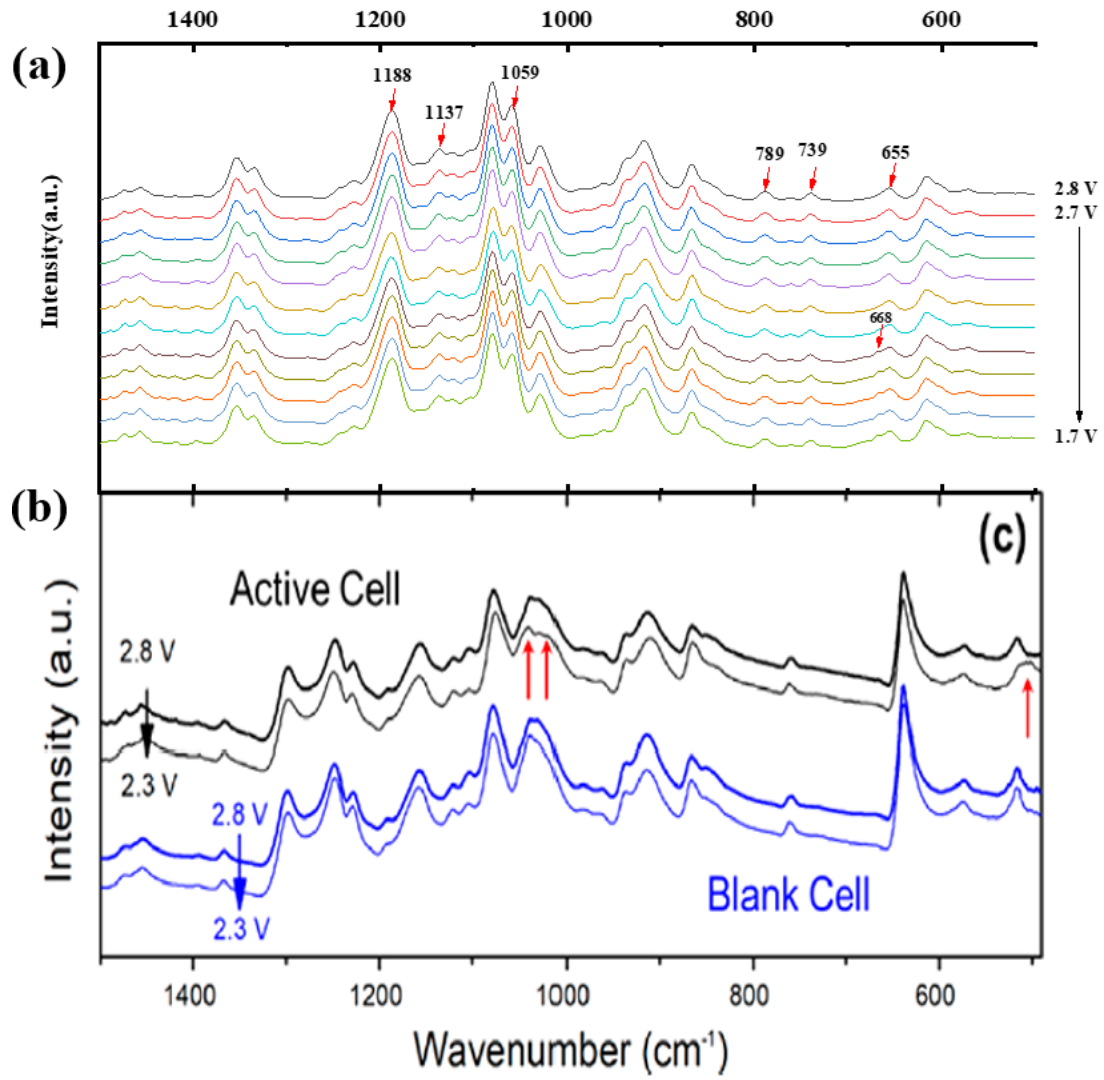


Fig. S16. (a) The discharging FTIR spectra of the SN-CoSn@C NBs-assembled LSBs at 500-1500 cm⁻¹. (b) FTIR spectra from the blank cell in literature ¹. The adsorption peaks are pointed by the red arrows.

Table S2. FT-IR peak assignments in literature ¹.

Peak (cm ⁻¹)	Assignment	Species	Ref.
1298	$\nu_s(\text{SO}_3)$	ion pairs	1
1248	$\nu_{as}(\text{SO}_3)$	ion pairs	
1228	$\nu_s(\text{CF}_3)$	free triflate ion	
1188	$\nu_{as}(\text{SO}_2)$	triflate ion	2
1167	$\nu_{as}(\text{CF}_3)$	ion pairs	1
1158	$\nu_{as}(\text{CF}_3)$	free triflate ion	1

1137	ν (C-N)	ion pairs	3
1121	ν (C-O)	DOL, DME, and/or ROLi	1
1104	C-O	DME	
1080	C-O/CH ₂ rocking	DOL	
1059	$\nu_s(\text{SO}_3)$	ion aggregates	
1050		ion aggregates	
1040		ion pairs	
1030		free ions	
1015	C-O	DME, DOL	
936		DOL ring vibration	
913		CH ₂ rocking/C-O stretch	
868	δ (Li-O)	R-OLi edge groups	
789	$\nu_s(\text{Co-N})$	ion pairs	4
762	$\delta(\text{CF}_3)$	R-OLi edge groups	
		ion pairs	
		free ions	
739	$\nu(\text{Sn-N})$	ion pairs	5
668	$\nu_{\text{as}}(\text{Sn-N})$	ion pairs	
655	$\delta(\text{Sn-N})$	bending mode	
616	$\delta_s(\text{S=O})$	sulfone, S ₂ O ₃ ²⁻	
572	$\delta(\text{SO}_3)$	bending mode	
517	$\delta(\text{CF}_3)$	bending mode	
504	(S-S)	S _x ²⁻ (2 ≤ x ≤ 8)	

Table S3. Performance comparison with other electrodes reported in literature.

Material type	Initial capacity (mAh g ⁻¹)	High rate capacity (mAh g ⁻¹)	Capacity decay rate per cycle	Ref.
Co-NCNT@CF/S	1259/0.1 C	627/3 C	0.038%/3 C/500	⁶
S@CNTs/Co ₃ S ₄ @NC	1570/0.1 C	850/5 C	0.014%/5 C/1000	⁷
E-Co _x Sn _y /NC/S-3	1264/0.1 C	778/2 C	0.0377%/1 C/500	⁸
S-FeCoNi@C-CNB/S	1238 /0.1 C	676/1 C	0.049%/1 C/200	⁹
S/FeCo-C	1251.9/0.2 C	791.9/1 C	0.073%/1 C/500	¹⁰
E-CoFeCN@C/S	1226/0.1 C	899.5/1 C	0.048%/1 C/300	¹¹
S/CoFe ₂ O ₄ @C	1191/0.2 C	816/2 C	0.063%/2 C/500	¹²
NiCo ₂ S ₄ @MoS ₂ -S	1118/0.1 C	1200/5 C	0.12%/5 C/500	¹³
SN-CoSn@C NBs	1291/0.1 C	557.3/5 C	0.056%/5 C/800	This work

References

- 1 C. Dillard, A. Singh and V. Kalra, *The Journal of Physical Chemistry C*, 2018, **122**, 18195-18203.
- 2 A. Doron, P. Elad, E. Ran, S. Gregory, K. C. Scordilis, A John, J. Electrochem. Soc., 2009, **156**, 694-702.
- 3 S. Yao, C. Zhang, Y. He, Y. Li, Y. Wang, Y. Liang, X. Shen, T. Li, S. Qin and J. Xiang, *ACS Sustainable Chemistry & Engineering*, 2020, **8**, 7815-7824.
- 4 C. He, Y. Zhang, Y. Zhang, L. Zhao, L. P. Yuan, J. Zhang, J. Ma and J. S. Hu, *Angew Chem Int Ed Engl*, 2020, **59**, 4914-4919.
- 5 A. Andrea, K. Christian, N. Christine, N. Heinrich, S. Martin, S. Wolfgang, *Chem. Ber.* 1996, **129**, 175-89.
- 6 D. Wang, K. Ma, J. Hao, W. Zhang, C. Wang, C. Xu, H. Shi, Z. Ji, X. Yan and Y. Gu, *Nano Energy*, 2021, **89**, 106426-106436.
- 7 H. Zhang, M. Zou, W. Zhao, Y. Wang, Y. Chen, Y. Wu, L. Dai and A. Cao, *ACS Nano*, 2019, **13**, 3982-3991.
- 8 Z. Qiao, F. Zhou, Q. Zhang, F. Pei, H. Zheng, W. Xu, P. Liu, Y. Ma, Q. Xie, L. Wang, X. Fang and D.-L. Peng, *Energy Storage Mater.*, 2019, **23**, 62-71.

- 9 Y.-J. Wu, C.-H. Chen, S.-H. Lin, C.-L. Huang, Y.-X. Yeh, J.-Y. Tan, J.-T. Su, C.-T. Hsieh and S.-Y. Lu, *J. Mater. Chem. A*, 2021, **9**, 9028-9037.
- 10 H. Li, L. Fei, R. Zhang, S. Yu, Y. Zhang, L. Shu, Y. Li and Y. Wang, *J. Energy Chem.*, 2020, **49**, 339-347.
- 11 X. Cao, M. Zhang, F. Zhu and X. Zhang, *J. Alloys Compd.*, 2022, **895**, 162609-162619.
- 12 L.-L. Gu, J. Gao, C. Wang, S.-Y. Qiu, K.-X. Wang, X.-T. Gao, K.-N. Sun, P.-J. Zuo and X.-D. Zhu, *J. Mater. Chem. A*, 2020, **8**, 20604-20611.
- 13 L. Yan, Z. Zhang, F. Yu, J. Wang, T. Mei and X. Wang, *Electrochim. Acta*, 2021, **383**, 138268-138274.